JOURNAL OF AIRCRAFT
Vol. 40, No. 2, March–April 2003

Engineering Notes

ENGINEERING NOTES are short manuscripts describing new developments or important results of a preliminary nature. These Notes cannot exceed 6 manuscript pages and 3 figures; a page of text may be substituted for a figure and vice versa. After informal review by the editors, they may be published within a few months of the date of receipt. Style requirements are the same as for regular contributions (see inside back cover).

Pitching-Moment Change Caused by High-Lift Devices on Wing-Body Configurations

Gerard W. H. van Es*
Ossenland 11, 1991 CW Velserbroek, The Netherlands

Nomenclature

A	=	wing aspect ratio
C_L	=	tail-off lift coefficient
C_m	=	pitching-moment coefficient (tail-off)
C_{m0}	=	pitching-moment coefficient at zero lift
dC_m/dC_L	=	slope of pitching-moment coefficient with lift coefficient
$\Delta C_{L\alpha=0}$	=	change in lift coefficient at zero angle of attack caused by high-lift devices
ΔC_{m0}	=	change in pitching-moment coefficient at zero lift caused by high-lift devices
$\Delta(dC_m/dC_L)$	=	change in pitching-moment coefficient slope caused by high-lift devices
$\Lambda_{c/4}$	=	wing sweep at quarter-chord

Introduction

KNOWLEDGE of the change in pitching moment caused by high-lift devices is needed to calculate the horizontal tail load required to trim an aircraft. This trim load reduces the total lift and also the maximum lift coefficient of an aircraft. Standard handbook methods such as those presented in Refs. 1–3 do not provide simple methods for a rapid estimation of the change in pitching moment caused by high-lift devices. In this Note extensive wind-tunnel data of wing-body configurations with high-lift devices were analyzed. These data were then used to develop a simple empirical method, which allows for the rapid prediction of the change in pitching moment caused by high-lift devices.

Theory

The change in pitching moment caused by high-lift devices is a result of the change in pitching moment about the local aerodynamic centres of each spanwise wing section of the flapped part of the wing. For an unswept wing this is the total change in pitching moment caused by high-lift devices. In general, this change will be a nose-down pitching moment. For a swept wing the change in spanwise lift distribution by the high-lift devices also influences the change in the pitching moment. In general for highly swept wings (e.g., sweepback angles of 40 deg or more) this will give a nose-up contribution.

Received 31 March 2001; revision received 18 November 2002; accepted for publication 18 November 2002.

*Aeronautical Research Engineer. Senior Member AIAA.

Trailing-edge devices have a significant effect on the pitching moment in contrast to influence on pitching moment of leading-edge devices, which is normally small. A body (e.g., a fuselage) can have a significant interference effect on the pitching-moment change caused by high-lift devices.[4] This interference results in a fictitious increase of the flap span. In general, this fictitious increase is the highest for a high-wing configuration. The relative size of the gap between the inboard part of a trailing-edge device and the body is also important.[4] It is not easy to predict the interference effect. Therefore, only experimental data for wing-body configurations are used in the present paper.

It is assumed that C_m varies linearly with C_L:

$$C_m = C_{m0} + \left(\frac{dC_m}{dC_L}\right) C_L \tag{1}$$

This approximation is valid for configurations with and without high-lift devices deployed as illustrated in Fig. 1. For wings having considerable amount of sweepback (i.e., more than 40 deg), the range of C_L over which C_m is linear with C_L is reduced compared to wings with less sweepback.

Empirical Correlations

The experimental data used in the development of the empirical correlations were obtained from Refs. 5–19. Also some unpublished data were used. The wing-body arrangements in the wind-tunnel experiments vary from high-, mid-, and low-wing configurations. The wing angle of sweep ranges from 0 to 35 deg and the wing aspect ratio from 5 to 12. All experiments were conducted at Mach numbers lower than 0.25.

Data for wing-body configurations with both leading- and trailing-edge devices deployed, as well as only deployed trailing-edge devices, were used. Various types of high-lift devices were used in the wind-tunnel tests. Data of configurations with only leading-edge devices deployed were not considered in this paper.

The changes in C_{m0} and dC_m/dC_L in Eq. (1) caused by high-lift devices are given by ΔC_{m0} and $\Delta(dC_m/dC_L)$, respectively. Close

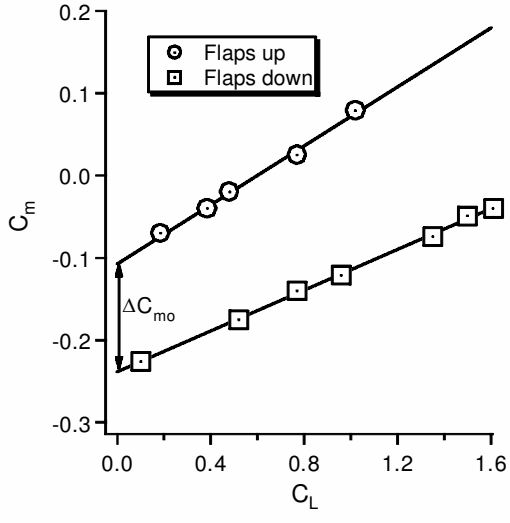

Fig. 1 Example of C_m vs C_L with and without high-lift devices for a Fokker F50 (Ref. 5).

examination of the experimental data showed that the influence of high-lift devices on $\Delta(dC_m/dC_L)$ was very small. This is in line with the theoretical results of Dent and Curtis.[20] For conceptual design purposes it can be assumed that $\Delta(dC_m/dC_L)$ is zero. The change in pitching moment caused by high-lift devices is then limited to a change in the zero-lift pitching moment only. Therefore empirical correlations were developed for the prediction of ΔC_{m0}.

At first a very simple correlation was considered. The lift increase caused by high-lift devices at zero angle of attack was correlated with the change in pitching moment. The result is shown in Fig. 2. All of the data showed a decrease in pitching moment with increasing lift. In the sign convention applied here, this means a nose-down pitching moment. Although a clear trend is visible in the data of Fig. 2, the scatter is still considerable. To reduce this scatter, a different correlation was considered. From theoretical methods (e.g., see Ref. 1) it is known that the change in pitching moment caused by high-lift devices is influenced by a number of variables. Wing sweep and wing aspect ratio are the most dominant variables. Therefore a correlation was developed between lift increase, wing sweep, and aspect ratio with the change in pitching moment. The following correlation was found from the experimental wind-tunnel data

$$\Delta C_{m0} = \left[-0.29 - 0.08A^{0.74}\tan(\Lambda_{c/4})\right](\Delta C_{L\alpha=0})^{1.1} \qquad (2)$$

Figure 3 shows the corresponding comparison between predicted and experimental values of ΔC_{m0}, where 85% of the data are correlated to within ± 0.09. The average error is ± 0.05. Therefore Eq. (2) gives an acceptable estimation of the magnitude of the pitching moment change at zero lift for conceptual design purposes. The change in lift coefficient caused by high-lift devices at zero angle of attack used in Eq. (2) can be estimated with standard handbook methods such as DATCOM (Ref. 1).

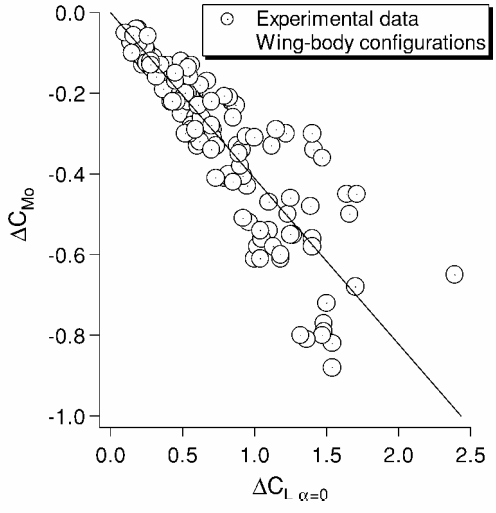

Fig. 2 Correlation between lift increase and pitching moment change caused by high-lift devices.

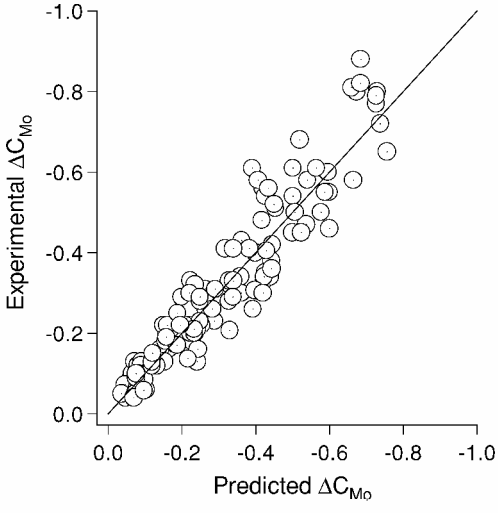

Fig. 3 Comparison of predicted and experimental values of ΔC_{m0} using Eq. (2).

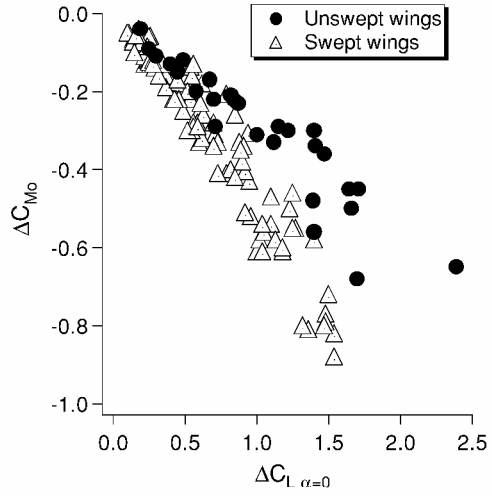

Fig. 4 Influence of wing sweep on pitching-moment change caused by high-lift devices.

Theoretical methods predict that for increasing sweepback angles the pitching-moment change becomes more nose up (e.g., see Refs. 1 and 20). The analyzed wind-tunnel data however showed an opposite trend, as is shown in Fig. 4. No explanation could be found for this difference between theory and experimental data. However in the development of Eq. (2), no data were used for configurations having wing sweepback angles above 35 deg. For wings having considerable amount of sweepback (i.e., more than 40 deg), the range of C_L over which C_m is linear with C_L is reduced compared to wings with less sweepback. Therefore Eq. (2) cannot be used for sweep angles higher than 40 deg.

Conclusions

A simple empirical method is presented for the prediction of the change in pitching moment caused by high-lift devices. The method is accurate enough to be used for conceptual design purposes.

References

[1]Finck, R. D., and Hoak, D. E., "USAF Stability and Control DATCOM," McDonnell-Douglas Corp., Long Beach, CA, 1978.

[2]"Aerofoil and Wing Pitching Moment Moefficient at Zero Angle of Attack due Deployment of Leading-edge High-Lift Devices," Engineering Sciences Data Unit, ESDU Item 00029, London, 2000.

[3]"Aerofoil and Wing Pitching Moment Coefficient at Zero Angle of Attack due Deployment of Trailing-Edge Double- and Triple Slotted Flaps at Low Speeds," Engineering Sciences Data Unit, ESDU Item 99014, London, 2000.

[4]"Information on the Use of Data Items on Flaps Including Estimation of the Effect of Fuselage Interference," Engineering Sciences Data Unit, ESDU Item 75013, London, 1990.

[5]Obert, E., "A Method for the Determination of the Effect of Propeller Slipstream on Static Longitudinal Stability and Control of Multi-Engined Aircraft," Delft Univ. of Technology, Faculty of Aerospace Engineering, Rept. LR-761, Delft, The Netherlands, 1994.

[6]Paulson, J. W., "Wind-Tunnel Results of the Aerodynamic Characteristics of a 1/8-Scale Model of a Twin Engine Short-Haul Transport," NASA-TM-X-74011, 1977.

[7]Paulson, J. W., and Morgan, H. L., "Aerodynamic Characteristics of Wing-Body Configuration with Two Advanced General Aviation Airfoil Sections and Simple Flap Systems," NASA-TN-D-8524, 1977.

[8]Hahne, D. E., and Jordan, F. L., "Full-Scale Semispan Tests of a Business-Jet Wing with a Natural Laminar Flow Airfoil," NASA-TP-3133, 1991.

[9]Comisarow, P., and Spearman, M. L., "An Investigation of the Low-Speed Static Stability Characteristics of Complete Models Having Sweptback and Sweptforward Wings," NACA-RM-L8H31, 1948.

[10]Carter, A. W., "Effects of Ground Proximity on the Longitudinal Aerodynamic Characteristics of an Unswept Aspect-Ratio-10 Wing," NASA-TN-D-5662, 1970.

[11]Lovell, D. A., "A Wind-Tunnel Investigation of the Effects of Flap Span and Deflection Angle, Wing Planform and a Body on the High-Lift Performance of a 28 degrees Swept Wing," Aeronautical Research Council, ARC CP-1372, London, 1977.

[12]Lovell, D. A., "A Low-Speed Wind-Tunnel Investigation of the Tailplane Effectiveness of a Model Representing the Airbus Type of Aircraft," Royal Aircraft Establishment, RAE Technical Rept. 69077, London, 1969.

[13]Kirby, D. A., and Hepworth, A. G., "Low-Speed Wind-Tunnel Tests of the Longitudinal Stability Characteristics of Some Swept-Wing Quiet Airbus Configurations," Royal Aircraft Establishment, RAE Technical Rept. 76029, London, 1976.

[14]Aiken, T. N., and Soderman, P. T., "Full-Scale Wind-Tunnel Tests of a Small Unpowered Jet Aircraft with a T-Tail," NASA-TN-D-6573, 1971.

[15]Aiken, T. N., and Page, V. R., "Stability And Control Characteristics of a Large Scale Deflected Slipstream STOL Model with a Wing of 5.7 Aspect Ratio," NASA-TN-D-6393, 1971.

[16]Page, V. R., Deckert, W. H., and Dickinson, S. O., "Large-Scale Wind-Tunnel Tests of a Deflected Slipstream STOL Model with Wings of Various Aspect Ratios," NASA-TN-D-4448, 1968.

[17]Gentry, G. L., Hammond, A. D., and Margason, R. J., "Longitudinal Stability and Control Characteristics of a Powered Model of a Twin-Propeller Deflected-Slipstream STOL Airplane Configuration," NASA-TN-D-3438, 1966.

[18]Page, V. R., and Weiberg, J. A., "Large-Scale Wind Tunnel Tests of a Airplane Model with an Unswept, Aspect-Ratio-10 Wing, Four Propellers, Blowing Flaps," NASA-TN-D-25, 1959.

[19]Chrisenberry, H. E., Doss, P. G., Kressly, A. E., Prichard, R. D., and Thorndike, C. S., "The Results of a Low Speed Wind Tunnel Test to Investigate the Effects of Installing Refan JT8D Engines on the McDonnell Douglas DC-9-30," NASA-CR-121220, 1973.

[20]Curtis, M. F., and Dent, M. M., "A Method of Estimating the Effect of Flaps on Pitching Moment and Lift on Tailless Aircraft," Royal Aircraft Establishment, RAE Rept. Aero 1861, London, 1943.

Euler Solutions for a Medium-Range Cargo Aircraft

Cengizhan Bahar,* Nafiz Alemdaroğlu,† and Yusuf Özyörük‡
Middle East Technical University, 06531 Ankara, Turkey
and
Emre Temel§
Aselsan, Inc., 06172 Ankara, Turkey

Introduction

COMPUTATIONAL fluid dynamics (CFD) has advanced rapidly as a discipline and is being increasingly used to complement the wind-tunnel measurements of complete aircraft configurations. Wind-tunnel tests are often limited by instrumentation constraints, precise model manufacturing, tunnel calibration, flow quality, wall and support interferences, and aeroelastic effects. Compared to wind-tunnel tests, CFD analyses are less expensive and require less time.

Received 6 January 2002; presented as Paper 2002-0402 at the AIAA 40th Aerospace Sciences Meeting and Exhibit, Reno, NV, 14–17 January 2002; revision received 20 October 2002; accepted for publication 2 December 2002.

*Graduate Student, Department of Aerospace Engineering; currently Engineer, Roketsan, Inc., Elmadag, 06780 Ankara, Turkey.
†Professor, Department of Aerospace Engineering. Member AIAA.
‡Associate Professor, Department of Aerospace Engineering.
§Engineer, MST Division, Systems Engineering Department, PK 101.

This Note focuses mainly on the modeling of complex, three-dimensional flowfields around a medium-range cargo aircraft, CN-235 (Ref. 1). Inviscid, subsonic flow solutions for the cargo aircraft were obtained at cruise and high-lift configurations using a commercial CFD code. The code is briefly described in the next section. The results are presented, and some conclusions are drawn from the study.

CFD Solver

Computations were done using the commercially available CFD-FASTRAN™ V2.2 code[2] employing unstructured grid methodology. The CFD-FASTRAN-V2.2 code is an implicit/explicit, upwind, cell-centered, Euler/Navier–Stokes flow solver based on finite volume method. Only the full-implicit scheme was used for all of the computations presented in this Note. The unstructured grids were generated using the commercial grid-generation code, CFD-GEOM™ V5, employing the advancing front method.[3,4] For computing flows over complex geometries, the use of unstructured grids offers considerable savings in the number of grid points and reduces the grid-generation time.[5] The geometry of the aircraft was modeled using the I-DEAS™ CAD tool.

Results and Discussion

The geometry of the conventional type, medium-range cargo aircraft, CN-235, is shown in Fig. 1. The solution model assumes no aileron, elevator, or rudder deflections. The landing gear and the propeller are also omitted, but the gondola and the engine nacelle (with blocked air intake) are retained. In the high-lift configuration study inboard and outboard wings with single-slotted flaps and flap-hinge fairings are also modeled. The overall length of the aircraft is 21.4 m, full wingspan is 25.81 m, and the root chord is 3.0 m. The aircraft has a cantilever high-wing monoplane and raked wing tips. The wing is set to a 3-deg incidence angle and has $NACA65_3$-218 wing sections.

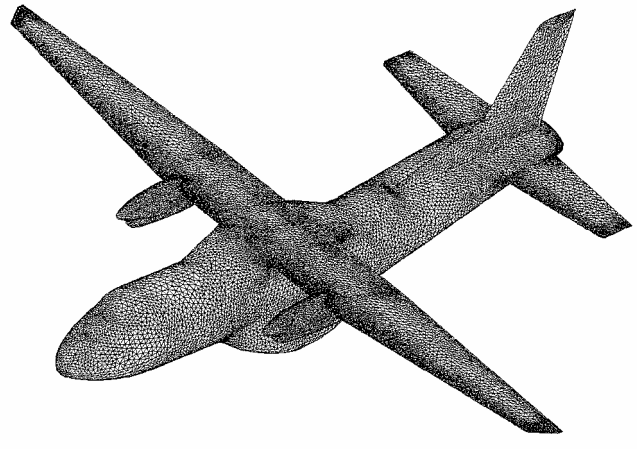

Fig. 1 Surface grid on the aircraft at cruise condition.

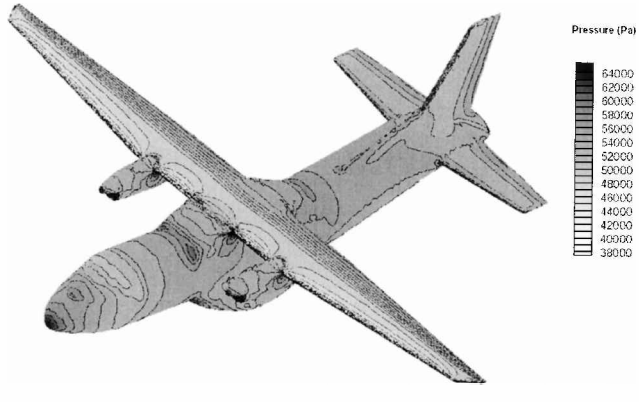

Fig. 2 Pressure contours on the aircraft at cruise condition, $\alpha = 5$ deg and $P_\infty = 57{,}207$ Pa.